



Table S1. Statistics of structures.

	AU ₆ A•Hfq65•A ₇	Hfq65•A ₇
Data collection		
Space group	I 1 2 1	C 1 2 1
Cell dimensions	 	
<i>a, b, c</i> (Å)	60.59, 38.28, 84.52	103.99, 40.71, 100.85
α, β, γ (°)	90.00, 90.00, 90.00	90.00, 101.36, 90.00
Resolution (Å)	30.3-1.80 (1.9-1.80) *	31.1-1.90 (2.03-1.90)*
<i>R</i> _{merge} (%)	5.7 (26.8)	5.9 (10.5)
<i>I</i> / σI	18.5 (2.7)	12.1 (6.2)
Completeness (%)	98.4 (99.0)	99.2 (100.0)
Redundancy	6.5 (6.6)	3.6 (3.6)
Wilson B factor (Å ²)	29.7	35.0
Refinement		
Resolution (Å)	30.3-1.80	31.1-1.90
No. reflections	17902	32695
<i>R</i> _{work} / <i>R</i> _{free} (%)	18.8/22.5	19.0/23.1
No. atoms	1842	3284
Protein	1489	2822
RNA	191	282
Water	162	180
<i>B</i> -factors (Å ²)		
Protein	15.25	16.14
RNA	22.97	30.04
Water	26.00	23.81
R.m.s. deviations		
Bond lengths (Å)	0.010	0.012
Bond angles (°)	1.5	1.3

*Values in parentheses are for highest-resolution shell.

Table S2. Sequence of RNA Oligonucleotides used in the study

Name	Sequence (5' to 3')
DsrAII	GGAAUUUUUAAGUGCUUCUUGCUUAAGCAAGUUUCA
rpoS-AA	GGGAACAACAAGAAGUUAAGGCGGGGCAAAAAAUA
rpoS-AC	AACAACAAG
A ₇	AAAAAAA
AU ₆ A	AUUUUUUA

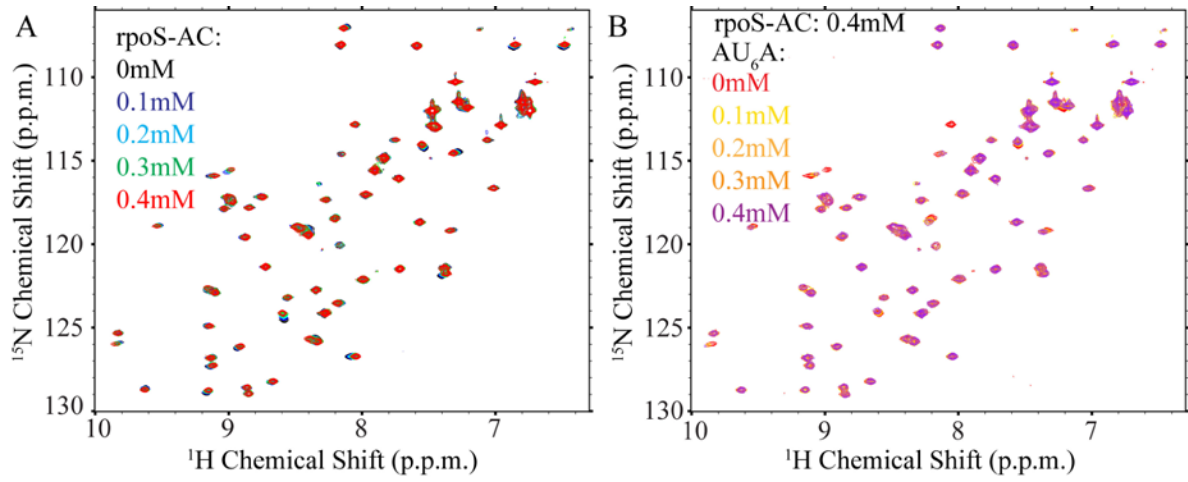


Figure S1. ^1H - ^{15}N spectrum of rpoS-AC followed by AU₆A titration to Hfq65 R16A/R17A.

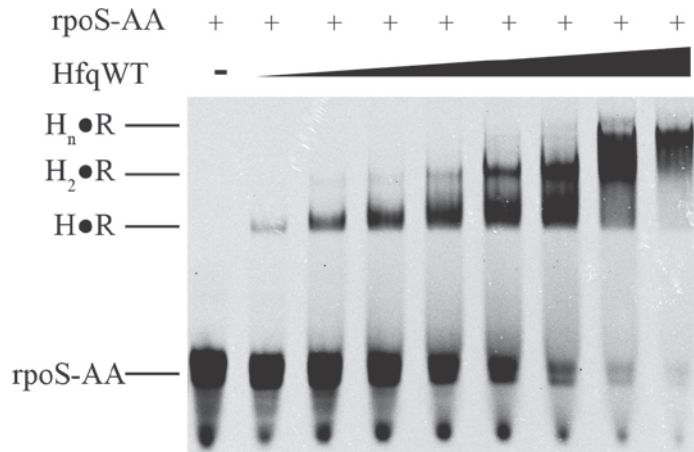


Figure S2. EMSA of rpoS-AA by wild-type Hfq.

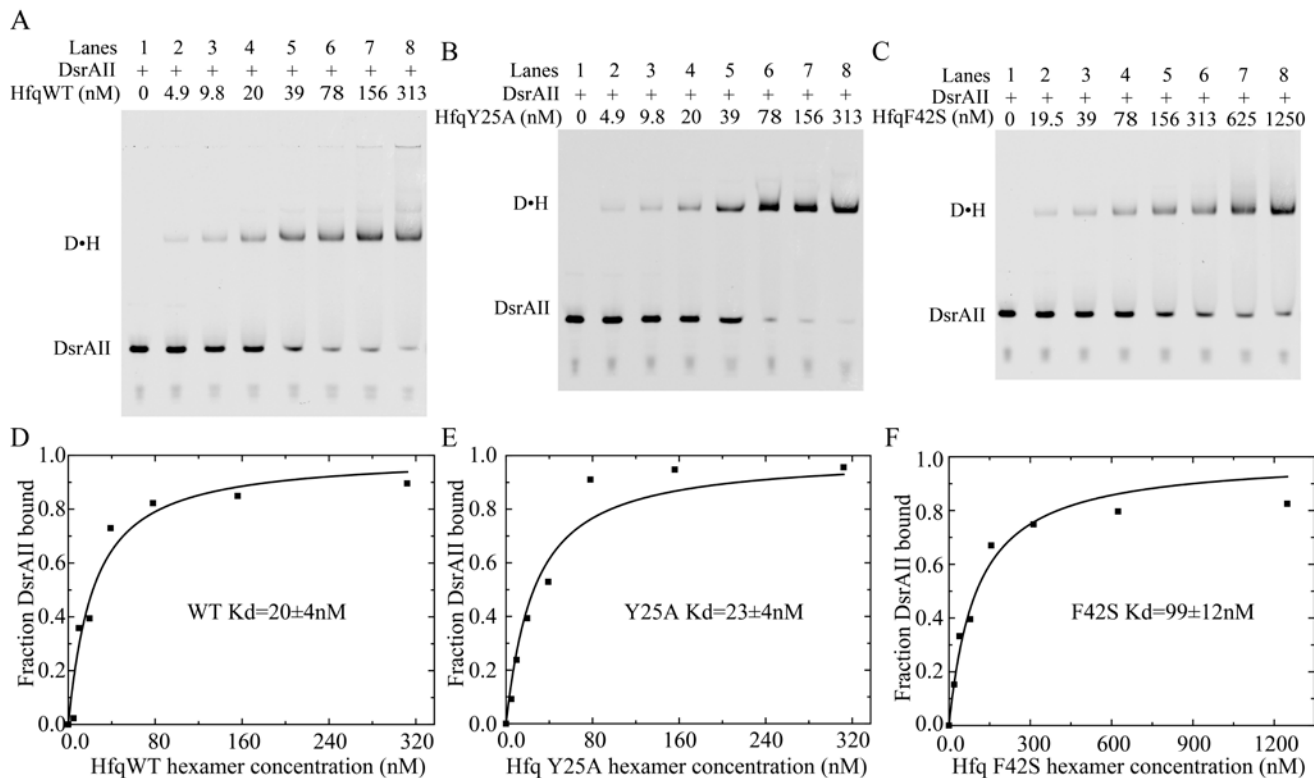


Figure S3. Binding affinities of DsrAII to HfqWT and mutants estimated from EMSA assays.

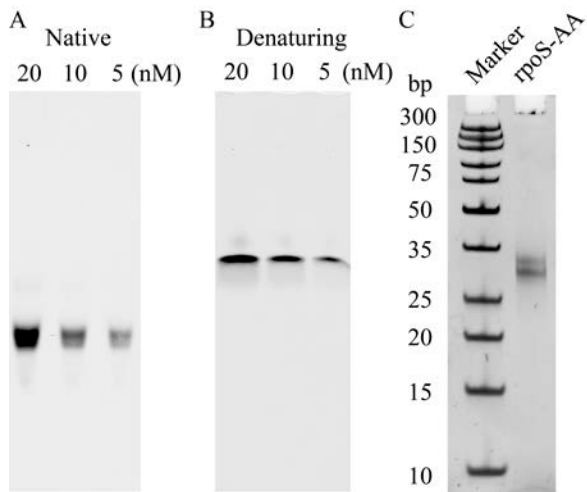


Figure S4. Different internal structures of rpoS-AA.

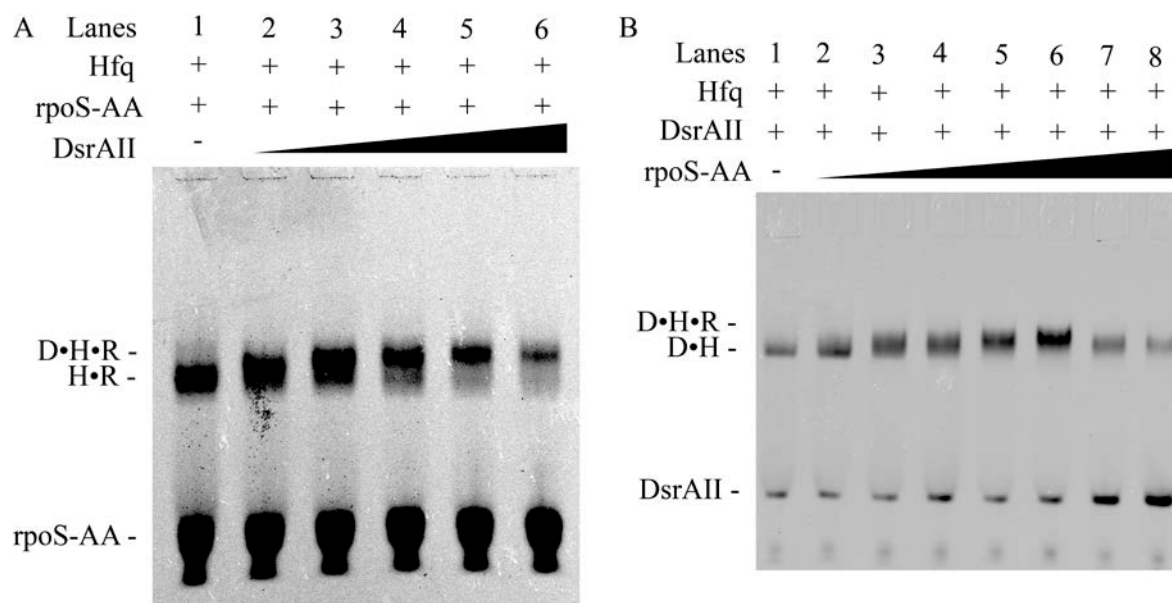


Figure S5. Full images of ternary complex EMSA.

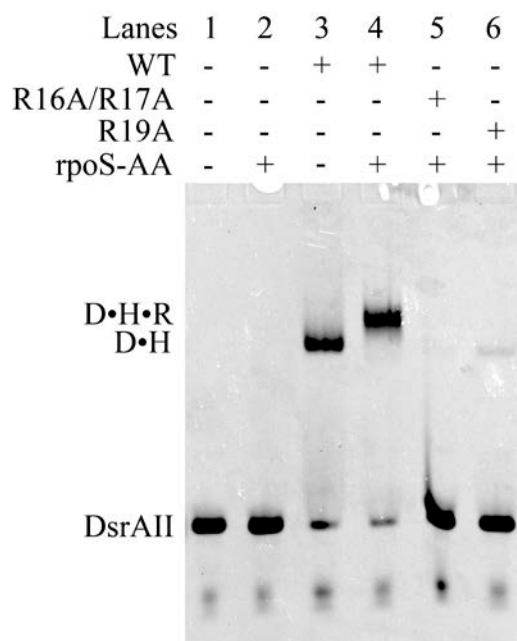


Figure S6. Lateral side mutations of Hfq abolish ternary complex formation.

Supplemental Figure Legends

Figure S1. ^1H - ^{15}N spectrum of rpoS-AC followed by AU₆A titration to Hfq65 R16A/R17A. (A) Titration of rpoS-AC into 0.1mM Hfq hexamer at 42°C. (B) AU₆A titration into sample containing 0.1mM Hfq and 0.4mM rpoS-AC. Spectra are overlaid with color codes presented in the figure.

Figure S2. EMSA of rpoS-AA by wild-type Hfq. 10nM labeled rpoS-AA was mixed with 9.8nM, 19.5nM, 39nM, 78nM, 156 nM, 312nM, 625nM and 1250 nM of Hfq hexamers. The mixture was resolved on a 6% native PAGE. With not more than 39nM Hfq, a 1:1 stoichiometry is dominant for Hfq•rpoS-AA complex. At higher Hfq concentrations, higher order complexes may form.

Figure S3. Binding affinities of DsrAII to Hfq wild type and mutants estimated from EMSA assays. Fluorescent intensities were integrated from EMSA images (A-C) to calculate bound fraction of labeled DsrAII. These intensities were fitted to 1:1 binding model (D-F). (A) and (D) Full length HfqWT binds to DsrAII at around 20nM Kd. (B) and (E) Hfq Y25A mutant binds to DsrAII with similar Kd (~23nM) as wild type. (C) and (F) F42S mutation increased Kd by ~5 folds, to a value of ~99nM.

Figure S4. Different internal structures of rpoS-AA. (A) The fluorescent labeled RNA fragment rpoS-AA ran as double bands on 6% native PAGE. (B) On 6% denaturing only one band was observed. (C) On 15% PAGE stained by Gel-Red, the two bands of rpoS-AA have similar apparent molecular weight.

Figure S5. Full images of ternary complex EMSA. (A) Super-shift of Hfq•rpoS-AA complex by DsrAII. Wild type HfqFL was mixed with fluorescent labeled rpoS-AA at final concentrations of 39nM and 10nM respectively. DsrAII concentrations in lanes 1 to 6 are 0nM, 7.8nM, 15.6nM, 31.3nM, 62.5nM and 125nM respectively. (B) Super-shift of Hfq•DsrAII complex by rpoS-AA. Wild type HfqFL was mixed with fluorescent labeled DsrAII at final concentrations of 78nM and 5nM respectively. rpoS-AA concentration in lanes 1 to 8 are 0nM, 7.8nM, 15.6nM, 31.3nM, 62.5nM, 125nM, 250nM and 500nM, respectively.

Figure S6. Lateral mutations of Hfq abolish ternary complex formation. Wild type Hfq can bridge DsrAII and rpoS-AA into ternary complex (Lane 4). Mutations of positively charged residues on the outer rim of Hfq to Ala prevented formation of Hfq-RNA complex (Lanes 5 and 6).